

Metallogenic model and prognosis of the Shuiyindong super-large strata-bound Carlin-type gold deposit, southwestern Guizhou Province, China

ZHANG Yu¹, XIA Yong^{1*}, SU Wenchao¹, TAO Yan¹, ZHANG Xingchun¹, LIU Jianzhong², and DENG Yiming³

¹ State Key Laboratory of Ore Deposit Geochemistry, Institute of Geochemistry, Chinese Academy of Sciences, Guiyang 550002, China

² Geological Party 105, Guizhou Provincial Bureau of Geology and Mineral Exploration & Development, Guiyang 550018, China

³ Zijin Mining Stock Company Limited, Guizhou, Zhenfeng 562200, China

* Corresponding author, E-mail: xiayong@vip.gyig.ac.cn

Received June 8, 2009; accepted July 15, 2009

© Science Press and Institute of Geochemistry, CAS and Springer-Verlag Berlin Heidelberg 2010

Abstract The Shuiyindong deposit is one of the largest (more than 100 tonnes of Au) and highest grade (more than 7×10^{-6} – 10×10^{-6}), strata-bound Carlin-type gold deposits in southwestern Guizhou Province, China. The deposit is controlled by both structure and favorable lithology. It is situated near the axis of the striking Huijiabao anticline and is hosted in bioclastic limestone of the Permian Longtan Formation. Gold mineralization occurred under low temperature with T_h of $220^\circ\text{C} \pm$ and is closely associated with decarbonation, silicification, sulfidation and dolomitization. The deposit has a characteristic elemental assemblage of Au-As-Hg-Tl. Studies of geochemistry and isotope compositions indicated that the ore-bearing materials and fluids of the gold deposit mainly originated from a plutonic source, and possess a mixing feature with the strata matter during transportation from mantle to crust. Fluid inclusions in vein quartz from the gold deposit are rich in volatile flux, indicating that metallogenic fluid is an overpressured one. The activity and geothermal state of the Earth's crust in the long period of time are favorable for the formation of overpressured fluids in a large area, and extensive structures would drive the fluids into ore-forming system and make gold deposits formed. The complexity of structural movement in the upper crust of southwestern Guizhou Province resulted in complicated gold mineralization. Through metallogenic prognosis and exploration, the proven reserves of the deposit increased by tens of tonnes of Au and the deposit has become a super-large strata-bound Carlin-type gold deposit.

Key words strata-bound Carlin-type gold deposit; metallogenic model; metallogenic prognosis; Shuiyindong; southwestern Guizhou Province

1 Introduction

The region of southwestern Guizhou, which is a region where the Carlin-type gold deposits were found for the earliest time in China, is an important component of the Yunnan-Guizhou-Guangxi “gold triangle” province. The Carlin-type gold deposits in this region can be classified as two types, i.e., the fault type and the strata-bound type, on the basis of their occurrence, shape and structural controls. The former type includes the Lannigou, Yata, Banqi, Zhimudang (the upper orebodies), etc. with gold ores mostly occurring in high-angle compresso-shear faults. The ore-hosted strata are generally Middle and Lower Triassic in age, ore-bearing rocks are dominated by muddy siltstones and silty mudstones. The strata-bound gold deposits

include the Shuiyindong, Taipingdong, Zhimudang (the lower orebodies), Getang, Nibao, etc. Gold ores are hosted mainly in the interbedded rupture zone at the karst discontinuity surface of the Upper-Lower Permian and the Upper Permian strata. The deposits are mostly concealed ones at depth, the orebodies occur as stratiform, stratoid and lenticular ones and are developed along the strata, characterized by multi-layer distribution. Ore-hosted rocks are mainly impure bioclastic limestones and carbonate rocks in organic-rich coal series formations, with obvious anticline ore-controlling features. The Shuiyindong gold deposit is one of the most important strata-bound Carlin-type gold deposits in the study region. Detailed studies in recent years have shed much light on the metallogenic mechanisms of the strata-bound Carlin-type gold deposits in the study region, promoted metallogenic prognosis and exploration, thus

making the Shuiyindong gold deposit become a typical super-large Carlin-type gold deposit. On the other hand, a great breakthrough has been made in metallogenic prognosis and exploration of strata-bound Carlin-type gold deposits on a regional scale.

2 Basic geological characteristics of the deposit

The Shuiyindong gold deposit in Zhenfeng County, Guizhou Province, is a super-large strata-bound Carlin-type gold deposit which has been discovered in recent years with relatively high grade and possesses reserves corresponding to those of a typical super-large strata-bound Carlin-type gold deposit. This gold deposit is located in the eastern segment of the Huijiabao anticline at the juncture between the southwestern margin of the Yangtze para-platform and the westward extension of the Youjiang fold zone of the South China fold system, con-

stituting, together with the large-sized Zhimudang and Taipingdong gold deposits, the Huijiabao gold ore belt (Fig. 1). The Shuiyindong gold deposit is controlled by the core structure of the Huijiabao anticline and favorable lithologic assemblages. Orebodies occur within the 300-m bounds near the axial part of the Huijiabao anticline as stratiform, stratoid and lenticular ones, with their attitude in consistency with the occurrence of the strata. In strike the orebodies wavelly plunge eastwards, in space the orebodies are characterized by a multi-orebody upper-and-down distribution pattern. There are two types of ore-hosted strata, i.e., structurally altered bodies (Sbt), which occur in the unconformable contact of the Maokou Formation as a suite of strongly altered structural breccias, and the Longtan Formation (P₃l), which is a suite of coal series strata. Fine clastic rocks contain carbonaceous claystones and coal seams, interbedded with bioclastic limestones.

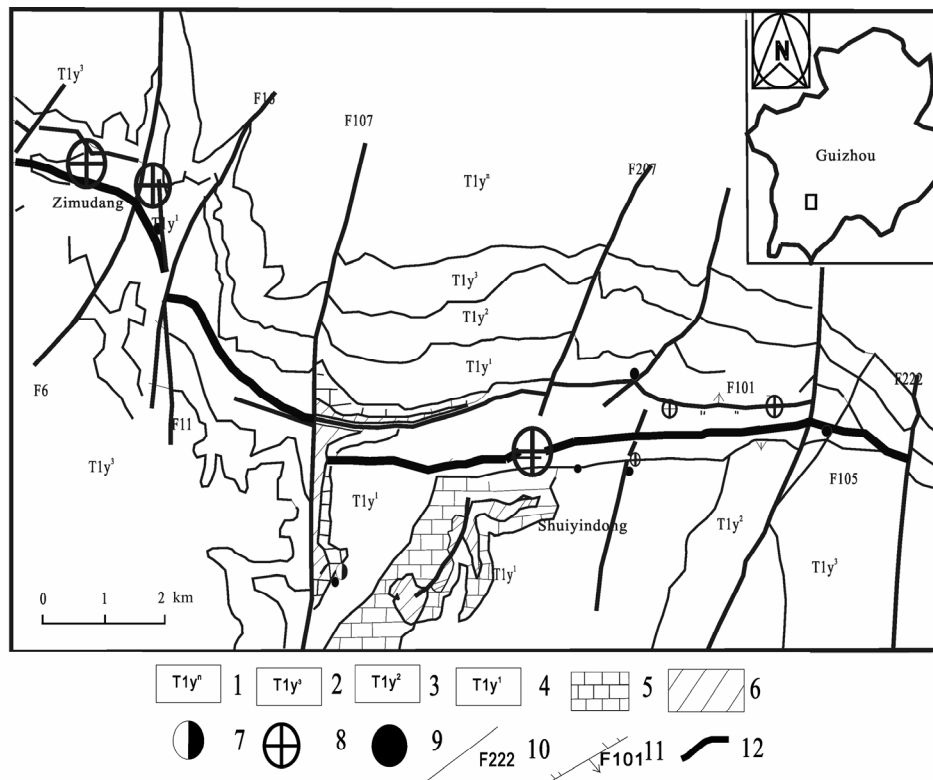


Fig. 1. Geological map of the Shuiyindong strata-bound Carlin-type gold deposit (Xia Yong, 2005; Su Wenchao et al., 2009). 1. Yonglinzhen Formation; 2. the third member of the Yelang Formation; 3. the second member of the Yelang Formation; 4. the first member of the Yelang Formation; 5. Changxing and Dalong formations; 6. Longtan Formation; 7. thallium-mercury deposit; 8. gold deposit; 9. mercury deposit; 10. normal fault and its number; 11. reverse fault and its number; 12. anticline axis.

Mineralized rocks are mainly composed of silicified dolomitized bioclastic limestones (Fig. 2). Wall-rock alterations are mainly silicification, dolomitization, pyritization, and secondly arsenopyritization, realgarization (orpimentization), clayization, fluoritization and other hydrothermal alterations. Of

the alterations, silicification, dolomitization, pyritization (associated with arsenopyritization) are most closely connected with gold mineralization. In the ores metallic minerals include pyrite, arsenopyrite, hematite, stibnite (occasionally seen), cinnabar (occasionally seen), realgar (occasionally seen), and native

gold (occasionally seen, found for the first time in this study) (Su Wenchao et al., 2006). Gangue minerals are quartz, dolomite, calcite, hydromica, sericite, kaolinite, and organic carbon. As viewed from the compositional

characteristics of ore minerals and phase analyses, it is known that pyrite and arsenopyrite are the carrier minerals of gold.

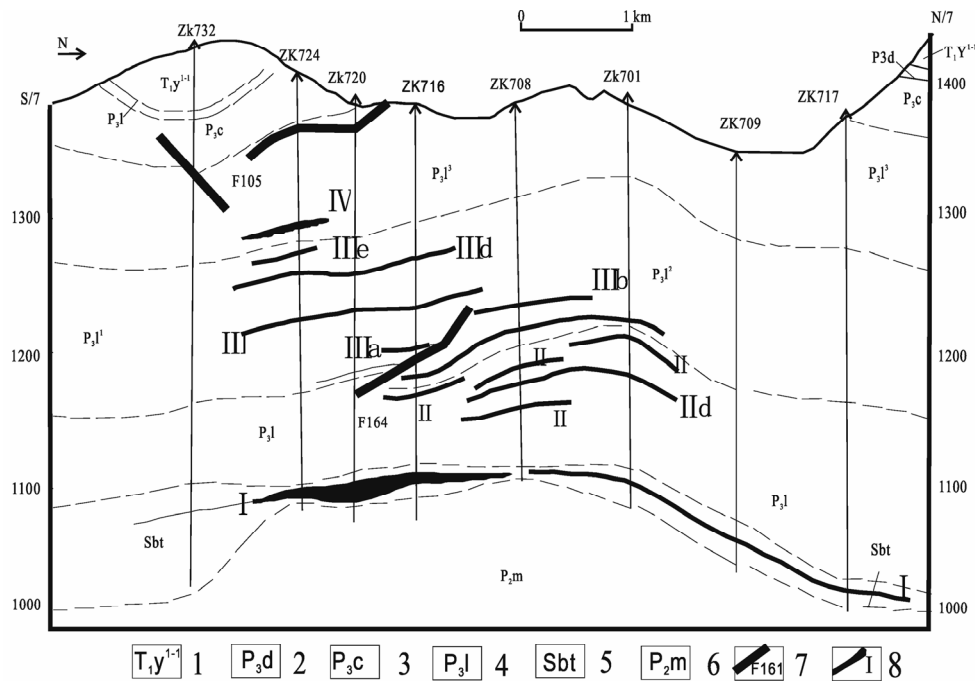


Fig. 2. Cross section of the Shuiyindong strata-bound Carlin-type gold deposit (Xia Yong, 2005; Liu Jianzhong et al., 2009). 1. The first member of the Yelang Formation; 2. Changxing Formation; 3. Dalong Formation; 4. Longtan Formation; 5. alteration zone; 6. Maokou Formation; 7. fault and its number; 8. gold orebody and its number.

Table 1. Average values of elements in ore-bearing rock series and content ratios of elements of normal rocks of the Shuiyindong gold deposit (unit: wt% for TiO₂, MnO, and 10⁻⁶ for the others)

Element	Average value of ore-bearing rocks/normal rocks				Element	Average value of ore-bearing rocks/normal rocks			
	Lime-stone	Muddy limestone	Claystone	Muddy silt-stone		Lime-stone	Muddy limestone	Claystone	Muddy silt-stone
Au	79.80	55.14	69.33	82.50	Zr	1.15	1.34	1.32	0.70
Sc	1.06	1.14	1.15	0.50	Nb	1.32	1.42	1.29	0.68
TiO ₂	1.25	1.04	1.19	0.62	Mo	1.59	6.56	1.42	1.48
V	0.65	1.46	1.23	0.66	Cd	1.87	2.76	2.67	6.31
Cr	0.55	2.32	1.01	0.54	Sn	0.57	2.20	1.79	0.97
MnO	1.25	1.69	0.45	1.20	Sb	2.91	7.95	11.73	32.80
Co	1.30	1.41	1.86	0.62	Cs	1.94	1.39	1.05	0.32
Ni	1.22	1.12	1.06	0.72	Ba	1.01	0.73	1.14	3.07
Cu	3.74	2.27	2.47	1.57	Hf	0.95	1.29	1.29	0.73
Zn	2.07	1.92	1.04	0.82	Ta	1.17	1.29	1.28	0.73
Ga	1.32	1.18	1.38	0.63	Tl	109.0	53.27	69.07	34.92
Ge	0.50	1.17	1.20	0.71	Pb	1.53	1.52	1.62	1.30
As	22.00	19.39	94.26	63.08	Th	0.96	1.04	1.21	0.79
Rb	1.60	1.14	1.51	0.87	U	0.70	3.34	1.47	2.01
Sr	0.25	0.60	0.51	0.86	REE	0.95	1.52	1.42	0.72
Y	0.84	1.61	1.31	0.74					

Note: Analyzed at the State Key Laboratory of Ore Deposit Geochemistry, Chinese Academy of Sciences by ICP-MS.

3 Geochemical characteristics of the deposit

3.1 Trace element geochemistry

Weakly altered or unaltered samples were selected from various types of rocks for trace element analysis and comparisons were made between their

trace element compositions with those of the same type of rocks in the ore-bearing series (Table 1).

As can be seen clearly, the contents of Au, As, Cu, Sb, Tl and Pb in the ore-bearing series are remarkably increased relative to those of unaltered rocks of the same type, reflecting that the trace elements had been brought in by mineralizing hydrothermal solutions. Ti, Sc, Nb, Ta, Zr, Hf, V, Cr, Co, Sn, Ga, Ge, Cd, Rb, Cs,

Ba, Mn, Zn, Th and REE showed a little variation in their contents. According to the element geochemical analysis, the former elements belong to the relatively inert elements without having been reworked by hydrothermal solutions, while the latter elements were affected by hydrothermal solutions, slightly influenced by hydrothermal superimposition and reworking processes.

There is no significant difference in primary contents of Au, As, Cu, Sb and Tl for various types of rocks (with unaltered rock samples for reference), and their variation is much less obvious than what was caused by mineralization alteration. As can be seen more clearly from the values of Table 1, the average contents of Au, As, Cu, Sb and Tl in various types of mineralized rocks are several tens to one hundred times those of the elements in the normal rocks of the same type. Of those elements, the contents of Au, As and Tl are the highest. It may be considered that the contents of these elements in the mineralized rock series were generally affected by mineralizing hydrothermal activities. Relatively speaking, their primary contents in the protoliths can be ignored. These elements are the basic hydrothermal elements in the Shuiyindong gold deposit. Their ratios can be used as the basic parameters for measuring the hydrothermal alteration intensity. As, Cu, Sb and Tl, especially As,

can be employed as the indicator elements for ore exploration.

3.2 Sulfur and lead isotope geochemistry

The analysis data (Table 2) showed that the sulfur isotopic composition of pyrite in the ore varies significantly, with $\delta^{34}\text{S}$ values varying within the range of +27.17‰– -8.64‰, with a range value of 35.81‰, indicating a high measure of dispersion. There would be shown the characteristics of sulfur of sedimentary origin and the involvement of other sources of sulfur. Electron microscopic analysis of pyrite monomineral (Fig. 3) indicated that pyrite in the ore contains framboid (irregular) pyrite powder crystals and zonal pyrite with thalheimite surface (hydrothermal origin) and framboid (irregular) pyrite core (primary sedimentary origin). The sulfur isotope values can only represent those of pyrite of primary sedimentary origin and hydrothermal origin. In most cases the volume of pyrite inner core (petrogenesis) is much larger than that of the girdles of thalheimite formed during the metallogenic period. Therefore, the sulfur isotope values obtained mainly represent the sulfur isotopic composition of pyrite of petrogenic origin, but can not fully represent the sulfur isotopic composition of ore-forming fluids.

Table 2. Results of the sulphur and lead isotope analysis for pyrite from the Shuiyindong gold deposit

Stratigraphy	$\delta^{34}\text{S}(\text{CDT})$	$^{206}\text{Pb}/^{204}\text{Pb}$	$^{207}\text{Pb}/^{204}\text{Pb}$	$^{208}\text{Pb}/^{204}\text{Pb}$	Model age (Ma)	ϕ	μ	$\Delta\beta$	$\Delta\gamma$
Ile	-0.43	18.361	15.56	38.452	153	0.582	9.39	15.003	26.208
IIf	-8.41	18.383	15.642	38.729	239	0.589	9.55	20.352	33.600
IIIa	5.72	18.304	15.54	38.501	169	0.583	9.36	13.699	27.515
IIIb (bottom)	8.16	18.145	15.551	38.382	300	0.595	9.4	14.416	24.339
IIIb (lower ore layer)	27.17	17.942	15.56	38.158	457	0.61	9.44	15.003	18.361
IIIb (upper ore layer)	21.11	18.452	15.532	38.332	49.1	0.573	9.33	13.177	23.005
IIf (parallel sample)	-8.64								

Note: $\Delta\beta = \frac{\beta - \beta_M}{\beta_M} \times 1000$; $\Delta\gamma = \frac{\gamma - \gamma_M}{\gamma_M} \times 1000$; $\beta = ^{207}\text{Pb}/^{204}\text{Pb}$ for samples; $\gamma = ^{208}\text{Pb}/^{204}\text{Pb}$ for samples; $\beta_M = ^{207}\text{Pb}/^{204}\text{Pb} = 15.33$ for the mantle;

$\gamma_M = ^{208}\text{Pb}/^{204}\text{Pb} = 37.47$ for the mantle. Analytical unit: Isotope Laboratory of Yichang Institute of Geology and Mineral Resources.

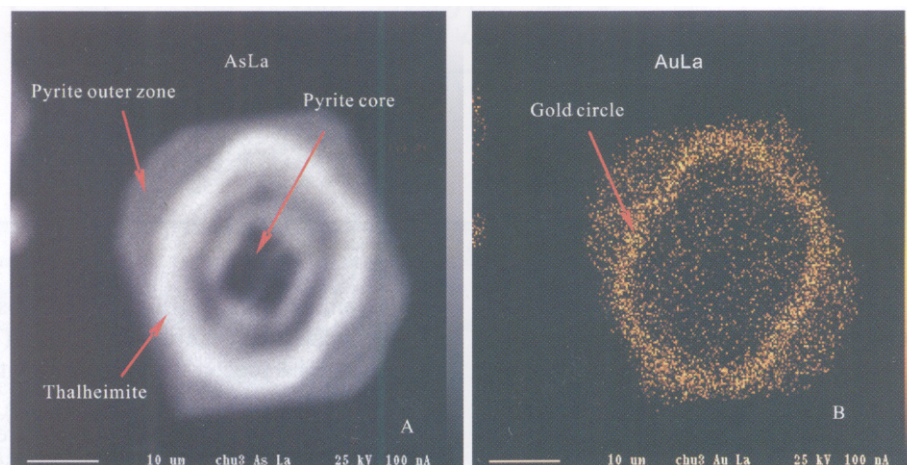


Fig. 3. Scan images of AsLa(A) and AuLa(B) compositions of fine-grained pyrite by electron microprobe spectral scanning.

Table 3. REE data ($\times 10^{-6}$) for calcite samples in the orebodies and wall rocks of the Shuiyindong gold deposit

Sample No.	La	Ce	Pr	Nd	Sm	Eu	Gd	Tb	Dy	Ho	Er	Tm	Yb	Lu
Cal-08	0.43	1.77	0.45	3.33	2.38	1.08	3.99	0.7	3.07	0.49	1.05	0.1	0.57	0.07
Cal-11	0.73	3.08	0.73	5.58	3.82	1.89	5.85	0.96	4.32	0.65	1.3	0.14	0.72	0.09
Cal-16	0.18	0.68	0.15	1.05	0.48	0.19	0.57	0.1	0.44	0.08	0.21	0.02	0.14	0.02
Cal-03	6.54	17.1	3.1	16.06	3.81	1.87	3.46	0.46	1.96	0.3	0.61	0.06	0.29	0.04
Cal-17	0.63	2.1	0.4	2.4	0.95	0.41	1.51	0.26	1	0.14	0.22	0.02	0.12	0.02
Cal-10	0.64	1.58	0.38	2.26	0.85	0.28	1.2	0.2	1.02	0.2	0.5	0.05	0.31	0.04
Cal-05	1.66	3.96	0.71	3.5	0.85	0.6	0.95	0.12	0.51	0.09	0.21	0.02	0.1	0.01
Cal-20	1.28	4.18	0.67	3.4	1.04	0.34	1.06	0.18	0.75	0.13	0.3	0.04	0.21	0.03
Cal-21	0.99	3.46	0.59	3.16	1	0.37	1.16	0.18	0.89	0.15	0.35	0.04	0.23	0.03
Cal-12	0.09	0.32	0.07	0.46	0.22	0.09	0.32	0.06	0.29	0.05	0.12	0.01	0.07	0.01
Cal-14	0.67	0.25	0.2	0.99	0.21	0.07	0.24	0.03	0.16	0.03	0.07	0.01	0.05	0.01
ZK1648-14	0.45	0.89	0.17	0.95	0.3	0.12	0.46	0.08	0.36	0.07	0.14	0.02	0.09	0.01
ZK3101-22	0.17	0.55	0.12	0.81	0.81	0.17	0.43	0.07	0.31	0.05	0.1	0.01	0.05	0.01
ZK2002-31	0.21	0.7	0.16	1.23	0.32	0.47	2.72	0.64	3.37	0.55	1.02	0.09	0.47	0.07
NN-03	2.06	3.1	0.49	2.357	0.565	0.182	0.961	0.171	1.009	0.221	0.609	0.085	0.5	0.074
NN-04	0.63	1.26	0.22	1.13	0.339	0.0178	0.45	0.064	0.361	0.068	0.149	0.018	0.087	0.011
NN-05-1	2.3	4.41	0.71	3.368	0.795	0.227	1.018	0.18	0.971	0.203	0.569	0.078	0.449	0.071
NN-05-2	1.49	2.47	0.34	1.234	0.2	0.046	0.192	0.032	0.189	0.036	0.103	0.015	0.087	0.013

From Su Wenchao et al., 2009.

Obvious variation is observed in the Pb isotopic composition of hydrothermal pyrite in the ores of the Shuiyindong gold deposit (Table 2), with the $^{206}\text{Pb}/^{204}\text{Pb}$, $^{207}\text{Pb}/^{204}\text{Pb}$ and $^{208}\text{Pb}/^{204}\text{Pb}$ values of 17.942–18.452, 15.532–15.642 and 38.158–38.729, respectively. The pyrite isotope data fall within the small triangle of normal lead, as is shown in the Cannon Pb isotope evolution diagram. It has been already identified that there are either normal lead or abnormal lead in the gold mining district of Southwest Guizhou (Liu Xianfan et al., 1997). The former is a mixture of single-source or multi-source lead. Country-rock strata or the samples which are closely associated with the strata are characterized by containing abnormal lead or high radiogenic lead (Faure, 1983; Zhang Qian et al., 2000). The variation of Pb isotopic composition of hydrothermal pyrite in the ores of the Shuiyindong gold deposit reflects that ore-forming materials may be of multi-source or mixing derivation.

3.3 The Sm-Nd isotopic composition of the Shuiyindong gold deposit and its ore-forming geochronological study

In the Carlin-type gold deposits there are usually no minerals suitable for traditional dating, so the problem of metallogenic time has not yet been solved. In the past the fission track method, the quartz fluid inclusion Rb-Sr method and the pyrite Pb-Pb method were used to constrain the metallogenic ages, giving a larger age range of 80–170 Ma (Hu Ruizhong et al., 2003). Studies by researchers from the Institute of Ore Deposits Geology showed that there are usually developed carbonate veins or realgar (orpiment)-stibnite-carbonate veins in the fault zones exposed on the surface or the hanging-wall of orebodies in the Carlin-type gold mining districts of Southwest Guizhou. The extensive development of such carbon-

ate veins may imply that there had occurred such geochemical processes as interactions between Au-bearing hydrothermal solutions and Fe-bearing carbonate strata or cements (decarbonation) and they would be the most direct macroscopic geological manifestation of decarbonation during gold metallogenesis.

REE analyses indicated that there are significant differences between the calcite veins closely associated with gold metallogenesis and those with no connection with gold metallogenesis on a regional scale (Su Wenchao et al., 2009) (Table 3, Figs. 4 and 5). The analytical results of Sm-Nd isotopic composition for calcite veins which have close genetic connections with gold mineralization are listed in Table 4 and the calculated results of Sm-Nd isotopic ages are shown in Fig. 6 (Su Wenchao et al., 2009). All the results showed that the considerably reliable mineralization age of the super-large Shuiyindong strata-bound Carlin-type gold deposit is 134–136 Ma (Early Cretaceous), just corresponding to the tectonic background of the regional lithosphere expansion.

3.4 Geochemistry of fluid inclusions

Fluid inclusions can be classified as two types: primary and secondary in accordance with their geneses. Primary fluid inclusions of quartz are characterized by isolated distribution and negative crystal shape. The inclusions are usually within the range of 5–60 μm , mostly 10–30 μm , in diameter. Secondary fluid inclusions are irregular or negatively crystalline, generally as large as 5–50 μm , mostly 10–50 μm in diameter. They are usually distributed along secondary fissures or are of curved distribution, but pyrite, arsenopyrite, stibnite, realgar (orpiment) and other sulfides are usually seen in secondary fissures, reflecting many times of tension and cracking following the formation of early quartz. These fluid inclusions dis-

tributed along the secondary fissures should preserve information about ore-forming fluids (Su Wenchao et al., 2001).

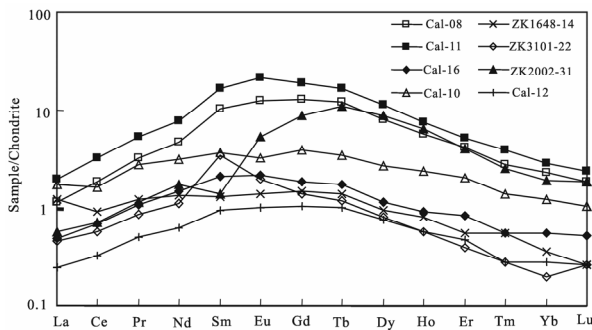


Fig. 4. The chondrite-normalized REE patterns for the calcite veins associated with Au mineralization in the Shuiyindong gold deposit. All data are normalized according to the chondrite REE values of Sun and McDonough (1989).

According to the phase-state characteristics of inclusions at room temperature (25°C) and their transformation in the process of freezing, liquid [CH₄-N₂-CO₂(LCH₄+N₂+CO₂)], gas [CH₄-N₂-CO₂(VCH₄+N₂+CO₂)], gas-liquid (VCH₄+N₂+CO₂+H₂O), CO₂-rich and gas-liquid inclusions can be classified. These inclusions usually coexist within one plane or

in fissures, implying that they once experienced immiscibility (Fig. 10).

Liquid [CH₄-N₂-CO₂(LCH₄+N₂+CO₂)] inclusions (Fig. 7) are dominated by primary fluid inclusions, and they are isolated in state and negatively crystalline, usually as large as 10–40 μm in diameter. In the process of heating, inclusions of this type would undergo decrepitation easily, indicating their high internal pressure.

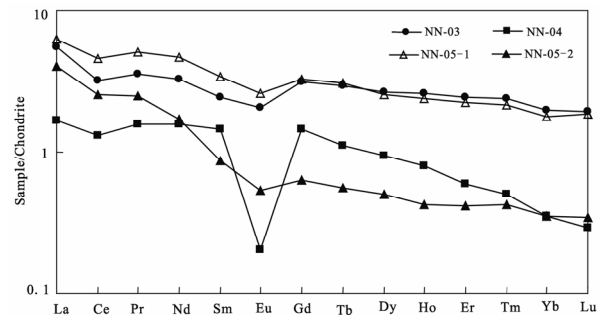


Fig. 5. The chondrite-normalized REE patterns for the calcite veins which have no genetic connection with gold mineralization. All the data are normalized according to the chondrite REE values of Sun and McDonough (1989).

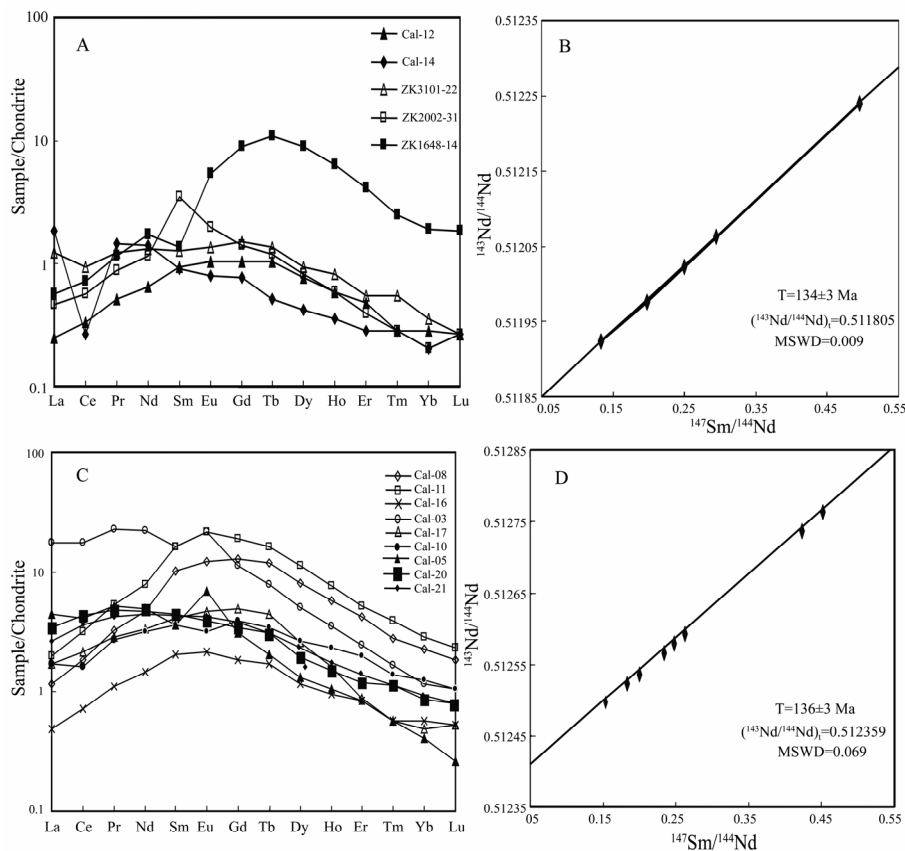
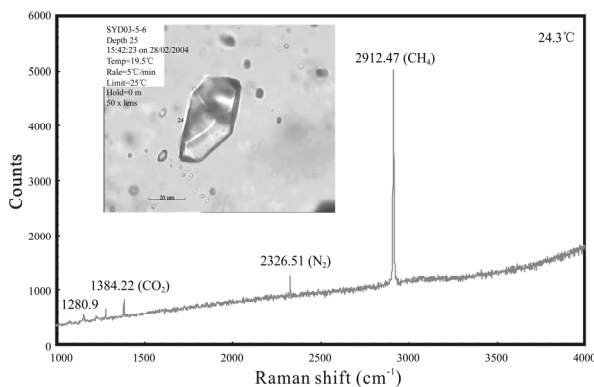
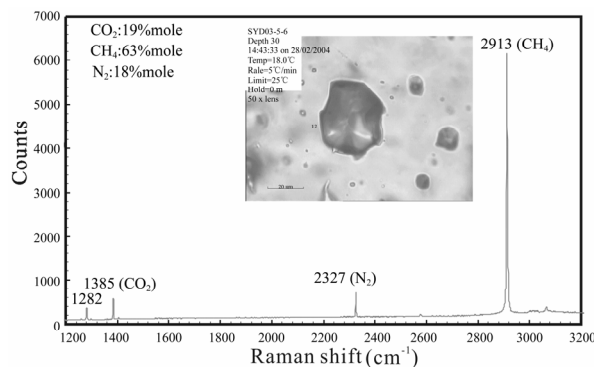


Fig. 6. The chondrite-normalized REE patterns (A and C) and corresponding Sm-Nd isochron ages (B and D) for the calcite veins from the Shuiyindong gold deposit. All the data are normalized according to the chondrite REE values of Sun and McDonough (1989).

Table 4. Sm, Nd and Sr isotopic compositions of calcite veins from the Shuiyindong gold deposit

Sample No.	Sm ($\times 10^{-6}$)	Nd ($\times 10^{-6}$)	$^{147}\text{Sm}/^{144}\text{Nd}$ (atomic)	$^{143}\text{Nd}/^{144}\text{Nd}$ (2σ) (atomic)	$^{87}\text{Sr}/^{86}\text{Sr}$ (2σ)
Cal-08	2.3002	3.0752	0.4522	0.512762 \pm 6	0.707083 \pm 10
Cal-11	3.8689	5.5334	0.4227	0.512735 \pm 5	0.707203 \pm 21
Cal-16	0.4683	1.0775	0.2628	0.512593 \pm 9	0.707482 \pm 13
Cal-03	3.6978	14.5286	0.1539	0.512496 \pm 7	0.707251 \pm 25
Cal-17	0.9178	2.2416	0.2475	0.512579 \pm 6	0.707991 \pm 11
Cal-10	0.8437	2.1825	0.2337	0.512567 \pm 8	0.707217 \pm 13
Cal-05	0.8203	3.2117	0.1544	0.512497 \pm 8	0.707152 \pm 16
Cal-20	0.9776	3.2226	0.1834	0.512523 \pm 12	0.707125 \pm 13
Cal-21	0.9602	2.8964	0.2004	0.512537 \pm 7	0.707143 \pm 10
Cal-12	0.2227	0.457	0.2946	0.512064 \pm 6	0.707729 \pm 8
Cal-14	0.2044	0.9306	0.1328	0.511922 \pm 15	0.707614 \pm 10
ZK1648-14	0.2869	0.8801	0.1971	0.511978 \pm 20	0.708003 \pm 24
ZK3101-22	0.812	0.9904	0.4957	0.512241 \pm 18	0.707610 \pm 11
ZK2002-31	0.39	0.9459	0.2493	0.512024 \pm 7	0.706620 \pm 18

From Su Wencho et al., 2009.

Fig. 7. Liquid [$\text{CH}_4\text{-N}_2\text{-CO}_2$ ($\text{L}_{\text{CH}_4+\text{N}_2+\text{CO}_2}$)] inclusions and their Laser Raman spectra.Fig. 8. Gas [$\text{CH}_4\text{-N}_2\text{-CO}_2$ ($\text{L}_{\text{CH}_4+\text{N}_2+\text{CO}_2}$)] inclusions and their Laser Raman spectra.

Gas [$\text{CH}_4\text{-N}_2\text{-CO}_2$ ($\text{V}_{\text{CH}_4+\text{N}_2+\text{CO}_2+\text{H}_2\text{O}}$)] inclusions (Fig. 8): Inclusions of this type are usually semi-transparent-black and mostly isolated and negatively crystalline, as large as 10–40 μm in diameter. Microthermometry and Laser Raman spectral studies revealed that inclusions of this type consist mainly of methane (CH_4) with high N_2 and CO_2 .

Gas-liquid [$\text{V}_{\text{CH}_4+\text{N}_2+\text{CO}_2+\text{H}_2\text{O}}$] inclusions (Fig. 9): At room temperature (25°C), fluid inclusions of this type are usually composed of one gas phase (V) and one liquid phase (L). Laser Raman spectral studies showed that the gas phase composition of this type of

fluid inclusions are mainly CH_4 , N_2 and CO_2 .

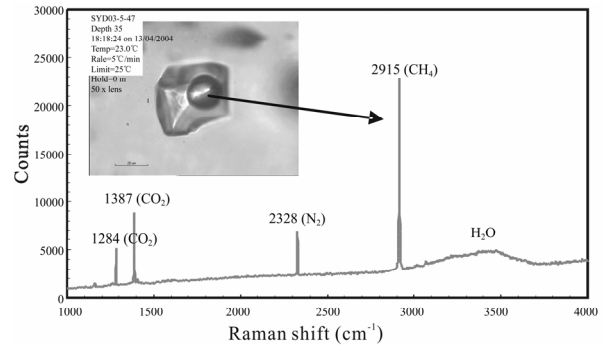
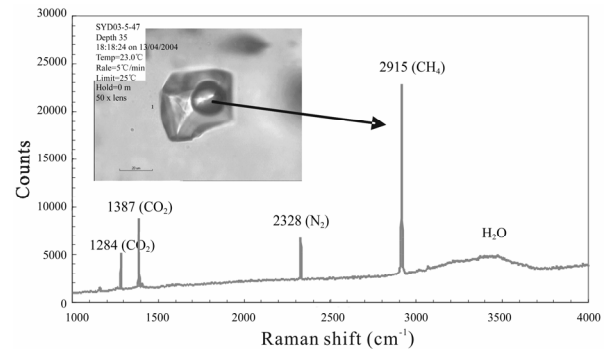
Fig. 9. Gas-liquid [$\text{V}_{\text{CH}_4+\text{N}_2+\text{CO}_2+\text{H}_2\text{O}}$] inclusions and their Laser Raman spectra.

Fig. 10. Various types of primary fluid inclusions intergrowing in a plane or fissures, showing the immiscibility features of fluids.

Results of microthermometric measurement for nearly 200 fluid inclusions indicated that the homogenization temperatures of [$\text{V}_{\text{CH}_4+\text{N}_2+\text{CO}_2+\text{H}_2\text{O}}$] fluid inclusions trapped during the metallogenic stage are within the range of 200–220 $^\circ\text{C}$ with the salinity of 5 wt%–6 wt% NaCl; CO_2 -rich fluid inclusions intergrown with [$\text{V}_{\text{CH}_4+\text{N}_2+\text{CO}_2+\text{H}_2\text{O}}$] fluid inclusions also have the same homogenization temperature range (200–220 $^\circ\text{C}$), probably implying that ore fluids experienced relatively reducing to oxidizing evolution processes. Changes in physical and chemical conditions of ore fluids may be the important factor leading to gold deposition. Preliminary pressure calculations indicated that the ore fluids had extremely high pressure [$(1.6\pm 0.4)\times 10^8$ Pa], corresponding to the lithostatic pressure at the depth of 6.4 \pm 1.6 km. The Triassic, Jurassic and Cretaceous strata in the region of Southwest Guizhou are about 4 km in thickness, indicating fluid pressure is higher than lithostatic pressure, showing the nature of overpressured fluids. In the relatively sealed structural system (e.g. overthrust fault), the abnormal overpressure of ore fluids can drive fluids to move laterally and infiltrate. Due to the higher pressure, the rocks would suffer hydrodynamic fragmentation, thus leading to such hydrothermal alterations as silicification and dolomitization

of country rock strata on a certain scale, forming such a spatial distribution pattern as the Shuiyindong-type fault-strata composite ore controlling. At the same time, rapid movement and release of overpressured fluids may be the important mechanism of gold deposition. Therefore, extensive silicification, dolomitization and other hydrothermal alterations are the important ore-search indicators of the Shuiyindong Carlin-type gold deposit in the field.

4 Metallogenic model

Through comprehensive geological-geochemical studies and discussion on the problems concerning metallogenesis, the metallogenic model of the Shuiyindong gold deposit can be summarized as follows:

Late Indosinian to Early Yanshanian tectonic movements put the end to the history of basin evolution in this region. Development of strata folds, faults, deep giant faults and magmatism, abnormally high geothermal temperature, and deeper burial resulted in the formation of ore fluids with abundant volatile elements in the deep interior of the crust and upper mantle. In addition, the fluids also became the overpressured fluids after extracting ore-forming elements in the Au-, Hg-, Sb-, As- and Tl-rich rocks in the basement and at great depth (Hu Ruizhong et al., 2003).

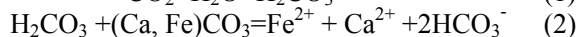
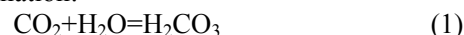
At that time, as the crust was in the compressive sealed stress state, the overpressured ore fluids were sealed at depth and were in strong equilibrium with the lithosphere. During the Yanshanian period this region was in the extensional state. With the injection of alkaline ultrabasic dykes (tubes), resurival of the faults had occurred at the basement, which, together with cover-strata faults, cut through the crust. As a result, the sealing conditions of overpressured ore fluids were destroyed, the fault system, like a pump, made ore fluids find their way into the upper crust. Gold in the ore fluids would be rapidly precipitated and accumulated as gold deposits in the favorable loci where metallogenic conditions changed suddenly. Meanwhile, Hg, Sb, As, Tl and other ore-forming elements would be precipitated as ores in the proper locations. All these led to what we see today in Southwest Guizhou, where the Carlin-type gold deposits are characterized by close Au-Hg-Sb-As-Tl paragenesis or association on a regional scale, while various gold deposits show the phenomenon of differentiation. At that time, as for the Shuiyindong gold deposit, due to the formation of the Huijiabao short-axis anticline and that of the favorable Upper Permian Longtan Formation assemblage of claystone→bioclastic limestone→claystone, volatiles with abundant CH₄, N₂ and CO₂, which found their way into the anticline core along the karst and non-karst

unconformability at the bottom of the Longtan Formation, and gold overpressured ore fluids were gathered. The fluids contained no iron (Su Wenchao et al., 2006), gold can exist in the form of Au-S coordination compound (Seward, 1973; Hofstra and Cline, 2000; Zhang Jun et al., 2002). Relatively high pressure and high volatiles made ore fluids move laterally and infiltrate to some extent in bioclastic sandy limestones in the favorable lithologic assemblage. Sometimes, the overpressured ore fluids would hydrodynamically destroy the country rocks. With the structural development, the faults destroyed the traps constituted by the anticline and favorable lithologic assemblage, making volatiles in the fluids escape out rapidly. As a result, the fluid pressure dropped suddenly, followed by the decrease of reductivity and the local or partial involvement of iron, some other components and meteoric water in the strata, leading to significant differences in ore-forming conditions. The ore-forming conditions thus rapidly turned favorable for gold deposition, and gold would be rapidly precipitated with the crystallization of arsenopyrite (partly in the inner core of pyrite of sedimentary origin) or fine-grained cinnabar.

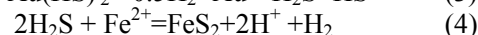
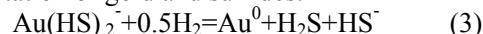
Run-through of the faults and the repeated occurrence of favorable lithologic assemblages led to the multi-layer orebody occurrence of the Shuiyindong gold deposit (Fig. 11). And Hg and Tl in metallogenic hydrothermal solutions possess much higher mobility, thus forming ore deposits in high-angle tensional-shear faults in the periphery of the gold deposit. Therefore, there appeared anticline core and low-angle compresso-shear fault strata-bound gold deposits and slightly later high-angle tensional-shear strata-bound Hg and Hg-Tl deposits.

Studies showed (Su Wenchao et al., 2006) that the mineralization experienced decarbonation, gold and sulfur precipitation and the formation of carbonate veins. The chemical reactions involved in these three processes are presented as follows:

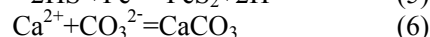
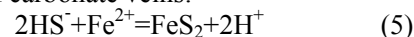
Decarbonation:



Precipitation of gold and sulfides:



Formation of carbonate veins:



a. Weak acidity of Au-bearing hydrothermal solutions made Fe-carbonate minerals in ore-hosted wall rocks dissolve, followed by the release of Fe and Ca into the hydrothermal system [Reactions (1) and (2)], i.e., decarbonation.

b. Au(HS)₂⁻ in hydrothermal solutions was decomposed under relatively reducing conditions,

making H_2S and HS^- enter into the hydrothermal system [Reaction (3)], both of them together with Fe-carbonate minerals were dissolved, releasing Fe^{2+} -bound pyrite (sulfidation) and producing H^+ [Reactions (4) and (5)]. The acidic environment resultant from sulfidation may further promote Fe-carbonate minerals in the wall rocks to dissolve, followed by the release of a large amount of Fe^{2+} into the hydrothermal system. Sulfidation would finally lead to the over-saturation of Au in hydrothermal solutions and its precipitation as native gold grains and accumulation on the surface of arsenopyrite grains or their margins.

c. Dissolution of Fe-carbonate minerals led to the release of Ca [Reaction (6)], which would be involved in the formation of late calcite veins, accompanied by Au pyrite veinlets or cutting through the latter. Therefore, high-grade Fe-carbonate ore-hosted wall rocks are one of the important factors for the formation of large-sized Carlin-type gold deposits. Carbonate veins associated with decarbonation may be one of the important indicators for search of large-sized Carlin-type gold deposits.

5 Metallogenic prognosis study and results

5.1 Main ore-search indicators

5.1.1 Structural indicators

The ore deposit is situated on the highest point of the regional short-axis Huijiabao anticline axis. Sbt and anticline structures ubiquitously existing in Southwest Guizhou are the good structural ore-search indicators. Faults are easy to form at the anticline axial part and become the channelways for the ascending of hydrothermal solutions or the loci where orebodies are emplaced.

5.1.2 Alteration indicators

Extensive decarbonation, fine disseminated pyritization, silicification and dolomitization are the alteration indicators for gold exploration. Wherever there occurs gold mineralization, there will be such alteration assemblages as mentioned above. The carbonate veins in close association with gold mineralization are the manifestation of decarbonation at depth on the Earth surface and also are one of the most important ore-search indicators for search of concealed Carlin-type gold deposits at depth.

5.1.3 Stratum lithological indicators

Carbonate rocks of the Longtan Formation of marine/terrestrial alternative phase are the stratum

lithological indicators for search of gold deposits like the Shuiyindong gold deposit, especially those alternative layers composed of thin carbonate rocks and thick clastic rocks. Fe-carbonate rocks are the most important ore-hosted wall rocks for the formation of high-grade, large-sized gold deposits.

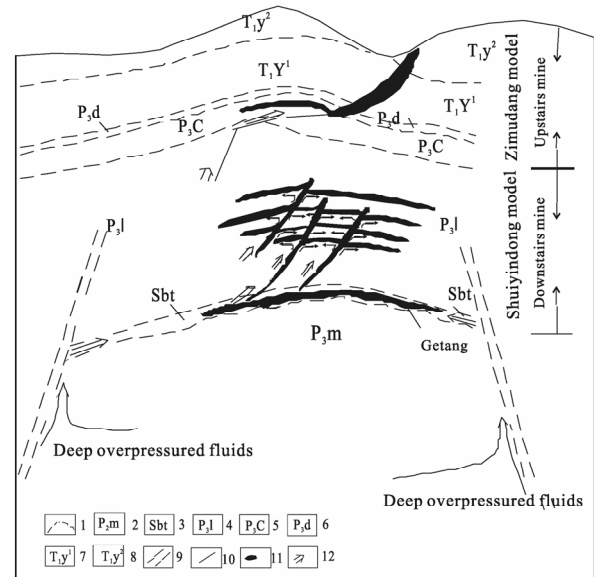


Fig. 11. The “two-stories” gold orebodies distribution and metallogenic model of the Shuiyindong strata-bound Carlin-type gold deposit (after Xia Yong, 2005). 1. Stratum boundary; 2. Maokou Formation; 3. alteration zone; 4. Longtan Formation; 5. Changxin Formation; 6. Dalong Formation; 7. the first member of the Yelang Formation; 8. the second member of the Yelang Formation; 9. deep giant fault; 10. fault; 11. gold orebody; 12. migration direction of ore-forming fluid.

5.1.4 Geochemical indicators

The element association of Au, Hg, As and Sb is distributed along the structurally axial line, indicating the rules of enrichment of gold and other ore-forming elements in favorable structural zones. There displays a close relation between Au and Hg, As, and Sb.

5.2 Extraction of metallogenic information and results of research on metallogenic prognosis

The ore deposit is controlled jointly by structure and favorable lithologic assemblage. Stratiform orebodies characterized by carbonate ore type were formed in the favorable strata of the anticline core. In low-angle faults and unconformable rupture zones were formed the fault-type orebodies characterized by the breccia-type ores. Hg ores or Hg-Tl ores occurred in the high-angle fault rupture zones in the periphery of the gold deposit. It is confirmed that the unconformable interface between P_{2m} and P_{3l} was the channel-

way for long-distance transport of ore-bearing hydrothermal solutions. Sbt is the product of regional structural hydrothermal activity and also the important locus of gold orebodies. Knowledge of these metallogenic rules and the mechanism of Au-Hg-As-Tl paragenesis-differentiation provides the theoretical basis for the extraction of metallogenic information at depth and the prognosis of metallogenic abnormalities of concealed strata-bound Carlin-type gold deposits and also points out the direction for search of concealed gold deposits in Southwest Guizhou.

According to the ore-search indicators provided in the project and the established metallogenic and ore-search model for the prognosis of good ore exploration prospects at the anticline axis in the eastern segment of the Shuiyindong gold mining district, the authors put forward the scheme of metallogenic prognosis with the aim to explore strata-bound gold orebodies by exploring along the eastward extensional region of the Huijiabao anticline axis and cutting through Sbt in the exploration project so as to enter the normal Maokou Formation as the end. Through recent several years of close collaboration with Geological Party 105 of Guizhou Provincial Bureau of Geological Resources Exploration and Development and Guizhou Zijin Gold Mining Stock Co. Ltd. for verification and reconnaissance of ore-search target areas, and gold orebodies buried at the depth of 300–800 m were discovered in the prospective areas of Xionghuangyan and Bojitian in the eastern segment of the Shuiyindong gold mining district. The deepest drilling reached 1411.08 m, and ores were still found in the structural alteration bodies on the unconformability at the depth of 1300 m and corresponding ore-hosted strata, thus making the reserves of the Shuiyindong gold deposit expand by several tens of tons of gold ores. It is also predicted that there are significant prospects for exploration of this type of gold deposits. The Shuiyindong gold deposit has become the first super-large strata-bound Carlin-type gold deposit in Southwest Guizhou.

Acknowledgements The project was supported jointly by the State Science and Technology Supporting Program (2006BAB01A13), the self-research project funded by the State Key Laboratory of Ore Deposit Geochemistry (Ore Deposit Special Research Project 2008.3-2), and Guizhou Provincial Bureau of Geology and Mineral Resource Exploration and Development [Qian Di Kuang Ke (2009) No. 11].

References

- Faure (1983) *Principles of Isotope Geology* (translated by Pan Shulan et al.) [M]. Science Press, Beijing.
- Hofstra A.H. and Cline J.S. (2000) Characteristics and models of Carlin-type gold deposits. In *Gold in 2000* (eds. Hagemann and Brown) [J]. *Reviews in Economic Geology*. **13**, 163–220.
- Hu Ruizhong, Su Wenchao, Bi Xianwu, Tu Guanchi, and Hofstra A.H. (2003) Geology and geochemistry of Carlin-type gold deposits in China [J]. *Mineralium Deposita*. **37**, 378–392.
- Liu Jianzhong, Chen Jinghe, Deng Yiming et al. (2009) Exploration practice of the Shuiyindong super-large gold deposit and new progress in exploration of the Huijiabao ore-concentrated area [J]. *Geology Survey and Research*. **32**, 138–143 (in Chinese with English abstract).
- Liu Xianfan, Liu Jiajun, Zhu Laimin, and Lu Qiuxia (1997) Pb isotope compositions and their application in Carlin-type gold deposits in Yunnan-Guizhou-Guangxi [J]. *Bulletin of Mineralogy, Petrology and Geochemistry*. **16**, 178–182 (in Chinese with English abstract).
- Seward T.M. (1973) The complexes of gold and the transport of gold in hydrothermal ore solutions [J]. *Geochim et Cosmochim. Acta*. **37**, 379–399.
- Su Wenchao, Hu Ruizhong, and Qi Liang (2001) Trace elements in fluid inclusions in the Carlin-type gold deposits, southwestern Guizhou Province [J]. *Chinese Journal of Geochemistry*. **20**, 233–239.
- Su Wenchao, Hu Ruizhong, Xia Bin, Xia Yong, and Liu Yuping (2009) Calcite Sm-Nd isochron age of the Shuiyindong Carlin-type gold deposit, Guizhou, China [J]. *Chemical Geology*. **258**, 269–274.
- Su Wenchao, Zhang Hongshu, Xia Bin, Zhang Xingchun, Hu Ruizhong, Zhou Guofu, and Xia Yong (2006) The first discovery of sub-micro and micro visible native gold grains in the Shuiyindong Carlin-type gold deposit in Guizhou [J]. *Acta Mineralogica Sinica*. **26**, 257–260 (in Chinese with English abstract).
- Su Wenchao, Zhang Hongtao, Xia Bin, Zhang Xingchun, Hu Ruizhong, Zhou Guofu, and Xia Yong (2006) Accumulation of visible gold in the Shuiyindong Carlin-type gold deposit [J]. *Acta Mineralogica Sinica*. **26**, 257–260 (in Chinese with English abstract).
- Sun S.S. and McDonough W.F. (1989) Chemical and isotopic systematics of oceanic basalts: Implication for the mantle composition and process. In *Magmatism in the Ocean Basins* (eds. Saunders A.D. and Norry M.J) [M]. Geological Society of London Special Publication, London. **42**, 313–345.
- Xia Yong (2005) *Study on the Metallogenic Characteristics and Gold Abnormal Enrichment Mechanism of the Shuiyindong Gold Deposit at Zhenfeng, Guizhou* [D]. Doctoral Dissertation of Post-graduate School of the Chinese Academy of Sciences.
- Zhang Jun, Lu Xinbiao, Yang Fengqing, Liao Qun'an, Wang Ping, Wang Keyong, Zhang Xiaojun, Wang Quanwei, Wang Hongmei, Chen Kanglin, and Fu Shaohong (2002) *Geology of Gold Deposits in Northwest China and Metallogenic Prognosis* [M]. Chinese University of Geology Press, Wuhan.
- Zhang Qian, Pan Jiayong, and Shao Shuxun (2000). An interpretation of ore lead sources from lead isotopic compositions of some ore deposits in China [J]. *Geochimica*. **29**, 231–2382 (in Chinese with English abstract).